The study aims to investigate the effect of Al_2O_3 and Al additions to Nickel-base superalloys as a coating layer on oxidation resistance, and structural behavior of nickel superalloys such as IN 738 LC. Nickel-base superalloys are popular as base materials for hot components in industrial gas turbines such as blades due to their superior mechanical performance and high-temperature oxidation resistance, but the combustion gases' existence generates hot oxidation at high temperatures for long durations of time, resulting in corrosion of turbine blades which lead to massive economic losses. Turbine blades used in Iraqi electrical gas power stations require costly maintenance using traditional processes regularly. These blades are made of nickel superalloys such as IN 738 LC(Inconel 738). Few scientists investigated the impact of Al_2O_3 or Al additions to Nickel-base superalloys as coating layer by using the slurry coating method on oxidation resistance to enhance the Nickel-base superalloy's oxidation resistance. In this study, IN 738 LC is coated with two different coating percentages, the first being (10 Al+90 Al_2O_3) and the second being (40 Al+60 Al_2O_3). Scanning Electron Microscope (SEM) and X-Ray Diffraction (XRD) were performed on all samples before and after oxidation. According to the results, SEM images of the surface revealed that the layer of the surface has a relatively moderated porosity value and that some of the coating layers contain micro-cracks. The best surface roughness of specimens coated with 60 % alumina+40 % aluminum was 5.752 nm. Whereas, the surface roughness of specimens coated with 90 % alumina+10 % aluminum was 6.367 nm. Results reveal that alloys with both Al_2O_3 and Al additions have reported a positive synergistic effect of the Al_2O_3 and Al additions on oxidation resistance. Moreover, the $NiCrAl_2O_3$ thermal coating has good oxidation resistance and the effective temperature of anti-oxidation is raised to 1100 °C in turn reducing the maintenance period of turbine blades

Keywords: slurry, coating, aluminizing, turbine blades, oxidation, IN 738 LC, superalloys, surface roughness

UDC 629
DOI: 10.15587/1729-4061.2022.259937

INVESTIGATION OF EVALUATED TEMPERATURE OXIDATION FOR IN-738 LC SUPERALLOY TURBINE BLADE THERMALLY COATED BY Al_2O_3 USING SLURRY COATING PROCESS

Naseer Abdulrazzaq Mousa
Lecture, MSc in Mechanical Engineering*
Bajel Mohammed Alshadeedi
Assistance Lecture, MSc in Mechanical Engineering*
Osam Hassan Attia
Corresponding author
Lecture, Doctor in Mechanical Engineering*
E-mail: osamhsattai@uobaghdad.edu.iq
Hussein Adel Mahmood
Lecture, Doctor in Mechanical Engineering*
Nor Mariah Adam
Professor, Doctor in Mechanical Engineering
Department of Chemical and Environmental Engineering
Faculty of engineering
Universiti Putra Malaysia
UPM Serdang, Selangor Darul Ehsan, Malaysia, 43400
*Department of Reconstruction and Projects
University of Baghdad
Karrada, Al-Jadriya, Baghdad, Iraq, 10071

Received date 11.04.2022
Accepted date 14.06.2022
Published date 30.06.2022

How to Cite: *Mousa, N. A., Alshadeedi, B. M., Attia, O. H., Mahmood, H. A., Adam,N. M. (2022). Investigation of evaluated temperature oxidation for IN-738 LC superalloy turbine blade thermally coated by Al_2O_3 using slurry coating process. Eastern-European Journal of Enterprise Technologies, 3 (12 (117)), 34–41. doi: https://doi.org/10.15587/1729-4061.2022.259937*

1. Introduction

Ni-based superalloys have been chosen to operate at high and elevated temperatures [1, 2]. Therefore, it should be enabled to maintain its hot corrosion, oxidation resistance, and strength to work at such high-level temperatures. In this consideration, alloying components such as (Al, Nb, Cr, Ti, Ta, W, Mo, Co) were added to the Ni matrix to improve the aforementioned characteristics of Ni-base superalloys. Among all other components, Al has a significant impact by constituting coherent precipitates (Ni_3Al ('phase)), which improves mechanical characteristics [3, 4]. Furthermore, Cr and Al can form protective oxides that enhance oxidation and hot corrosion resistance [5]. Though Al concentration in Ni-base superalloys has many benefits, high Al concentration in Ni-base superalloys can decrease the solubility of Cr in the Ni composite, resulting in a decrement in mechanical characteristics and hot corrosion resistance [6, 7]. In this respect, utilizing Coatings rich in Al may be a useful approach to prevent the bad impacts of Al in the bulk of Ni-base superalloys while improving corrosion and oxidation resistance. Nickel-base superalloys are popular as base materials for hot components in industrial gas turbines such as blades or vanes due to their superior mechanical performance and high-temperature

oxidation resistance [8]. On the other hand, the combustion gases' existence generates a harsh environment, as well as hot oxidation, which is inevitable when alloys are utilized at high temperatures for long durations of time [9]. Two approaches. Introducing a fair percentage of titanium, aluminum, and chromium, as well as minimal quantities of hafnium, zirconium, and yttrium to the alloy, can be used to enhance the mechanical and oxidation resistance of superalloys, the operational life of superalloy elements at high temperatures [10, 11]. Another method is to use various surface treatment techniques to coat the alloy with a protective layer. Pack cementation, plasma spraying, slurry process, and chemical vapour deposition are just a few of the coating methods that can be proposed [12, 13].

Protection coatings through slurry are frequently utilized in superalloys to safeguard against oxidation at high-temperature because this method is a cost-effective and efficiently managed surface safeguard strategy that co-deploys elements in components that have complex shapes and even porous structures for multi-component coatings [14, 15]. Seeking modern base substances and coatings for high-performance gas turbine engines is a significant step. Many developments in nickel-based superalloys are based on increasing the research area of thermal barrier coating (TBC) systems. Furthermore, the processing methods can offer the necessary coating characteristics for engine parts with complicated forms, like blades, turbine vanes, etc.[9].The study scope of electrodeposition has not been realized to a wide extent as an alternative to traditional strategies of generating bond coats as well as their effectiveness in increasing the life cycle. Due to their ability to create dense, adherent scales for Al_2O_3, Alumina coverings are commonly utilized as overlays and as a connection cover for TBCs on hot-gas turbine blades and other parts [16, 17]. At the present time, the running temperature of gas turbine engines is being raised in order to enhance their performance [18]. The availability of Al at the interface with the metallic coating for corresponding protection was depends on the formation a thin layer of Al_2O_3 [6].

2. Literature review and problem statement

The increased demand for high performance gas turbine engines has resulted in a continuous search for new base materials and coatings. With the significant developments in nickel-based superalloys, the quest for developments related to thermal barrier coating (TBC) systems is increasing rapidly and is considered a key area of research [19]. Gas turbine blades must be satisfying a life-time that reaches as high as 25000 h and, due to the fact that they have to withstand a variety of the degradation types (like the thermo-mechanical fatigue, creep, corrosion and oxidation) take place throughout service exposure to the aggressive environments, super alloys, or high efficiency alloys, are utilized as materials for making them up. Gas turbine blades for the land base power plants are constituted fundamentally of the Nickel-base super alloys, due to the fact that Ni has the ability for retaining higher strength levels at high temperatures compared to others. Slurry aluminide coating is considered one of the most excellent coating materials as absorbed from to enhance hot corrosion resistance for high temperature applications [20].

In [21], the authors looked into hot corrosion in the components of the gas turbine and came to a conclusion that it is one of the major causes of failure in gas turbine engines. For avoiding catastrophic failure, the hot corrosion should be completely avoided or recognized early, and the ultimate failure regarding turbine blades might be caused by a combination of the hot corrosion and an additional failure mechanism (for example, fatigue). While in [22], the researchers discovered that the Ni-based super alloy IN738 had higher creep resistance; nonetheless, the resistance to the oxidations is allo researchers that examined the behavior of Ni-based super alloys. Because of the low chromium content and high tungsten content, CM 247LC is easily corroded. In comparison to IN738LC, CM 247LC has larger cracks.

Vanadium is a trace element widely distributed in the Earth's crust. The anthropogenic sources of vanadium include fossil fuel combustion and wastes including steel industry slags. In fact, hot corrosion is a limiting factor for the life of components for gas turbines. Vanadium that is present in the fuel makes the corrosive by forming low melting point chemical compounds. In the vanadium environment there were fewer cracks and often no cracks than in the chloride environment and several cracks were found in coated samples. Coated MCrAlY IN738LC has a longer life compared to uncoated MCrAlY IN738LC It is found that heating of the coatings at 1100 °C leads to a diffusion redistribution of the elements over their thickness and the formation of a layered quasi-two-phase structure of Cr (in case Ni80Cr20 alloy) or Cr and Fe (in case Ni60Cr15 alloy) solid solutions in NiAl with different Al (Al-rich) and Ni (Ni-rich) saturations [26]. Also, the EDS data regarding a hot corroded CM247LC super alloy in a vanadium environment at 900° Celsius indicates larger levels of O, Ni, Na, Co, W and low amounts of Al, Cr, V and S. EDS data indicates larger levels of Na, O, S and Ni and low amounts of Cr, Co, Ti and Al in a hot corroded IN738LC super alloy in an environment of chloride at 900 °C. However, in [27], Spark plasma sintering regarding a multi-layer thermal barrier coating on Inconel738 super alloy was investigated by the researchers: They discovered a nano-structured Yttria – Stabilized Zirconia (YSZ) coating on an Ni-based super alloy (INCONEL738) with functionally-graded structure using spark plasma sintering (SPS). Under a vacuum atmosphere, a stack layer of INCONEL738/NiCrAlY powder/Aluminum foil/NiCrAlYYSZ powder/YSZ powder has been Spark Plasma Sintering (SPS) in a graphite die at a 40 MPa (8 Pa) applied pressure. In addition, sintering was carried out at a temperature of 1040 °C. Also, the TBC was prepared using air plasma spray (APS) process for comparison purposes. In spite of that, A metallographic analysis, hardness and strength measurements were carried out using the small punch test to locally study the mechanical properties of the coating surface [28].

Finally; IN-738 LC super alloys with slurry coating method used Al_2O_3 or Al additions on oxidation resistance required more investigation at high oxidation temperature for enhancement NiCe-Al_2O_3 oxidation resistance. Therefore, it presents research looked into superalloy IN-738 LC of these various turbine blades which used in power electric generation with enhancement the oxidation resistance at high temperature (1000 and 1100 °C)of the blade by coated it with a protective coating layer. While, effect of Al_2O_3 and Al additions on oxidation resistance. Additionally, two coating ratio of aluminized coating (10 Al+90 Al_2O_3) with that of the (40 Al+60 Al_2O_3).

3. The aim and objectives of the study

The aim of the study is to use the slurry coating method to applicate the coating layer for IN-738 LC super alloys with

slurry coating method used Al_2O_3 or Al additions on oxidation resistance required more investigation at high oxidation temperature for enhancement NiCe-Al_2O_3 oxidation resistance.

The following objectives have been set to achieve the aim:

– studying the structural behavior of the coating layer during isothermal cyclic oxidation;

– studying the effect of Al_2O_3 and Al additions on oxidation resistance;

– comparing the oxidation resistance of the aluminized coating (10 Al+90 Al_2O_3) with that of the (40 Al+60 Al_2O_3) coating.

4. Materials and methods

The slurry coating method was used to applicate the coating layer (Al_2O_3) in an attempt to enhance NiCeAl_2O_3 oxidation resistance. In the current study, the oxidation behavior at high temperatures with and without coatings was investigated. Furthermore, the primary objective of this research is to methodically analyze and evaluate oxidation resistance at the high temperature in superalloy IN-738 LC of these various blades. Superalloy was tested for high temperature cyclic oxidation.

This section involved two parts; the first part described several investigation tests that carried out on samples like: chemical composition analysis, optical microscope analysis, XRD, FE-SEM, EDX, AFM, X-Ray Diffraction(XRD) SHIMADZU LabX XRD-6000 Japan, the field emission scanning electron microscope (FE-SEM)SU9000 is HITACHI's new premium SEM, Energy Dispersive X-Ray(EDX)X'Pert^3 MRDMalvern Panalytical's Materials Research Diffractometers (MRD), Atomic Force Microscopy (AFM) Atomic Force Microscopy, Park, NX10, Koreahardness and coating thickness. The second part describes specimens preparation method for Slurry coating, Al powder is used in coating process.

The substrates employed in this research were nickel-based superalloy IN-738LC melted by the Institute of Chung Shan Science and Technology. Table 1 shows the chemical composition analysis of the used IN 738 LC.

Table 1 illustrates a very small difference between the chemical properties of the IN-738LC superalloy sample experimental and the standard composition. For the application of the coating layer, the slurry technique was used.

Utilizing a wire cutting machine with sizes of (20×15×2.5 mm) for prepared the test sample which collected from Baghdad gas electrical power plant supplied turbine blades, as shown in Fig. 1.

The samples are then cleaned with SiC (silicon carbide) papers (180, 220, 320, 400, 600, 800, 1000, 1200, 1500, 2000, 2500 μm) respectively from rough to smooth, then polished on very smooth surfaces. This is done through the use of a polishing machine model (MP-2B grinder- polisher).

For all coating specimens, a digital gage Type (TT260) is used to determine the thickness of the coating layer. Table 2 shows the coating thickness applied on the samples.

a *b*

Fig. 1. Turbine blades: *a* — turbine blade; *b* — prepared sample

Table 2

Coating Thickness

Coated Sample	Thickness measured by digital gage (μm)
IN 738 LC (10 Al+90 Al_2O_3)	215
IN 738 LC (40 Al+60 Al_2O_3)	198

The device has ±0.05 *mF*: ±(1μ+3 % *H*) *m* accuracy, where *H* is actual thickness tested and *F* is ferrous, from the other hand and according to this accuracy, measurements are taken in three locations to obtain an averaged thickness, but this device occasionally gives inaccurate readings, so SEM is used to determine thickness in the majority of cases. Using the Image J tool, two-dimensional SEM cross-sectional micrographs were used to measure the coating thickness.

Table 3 shows roughness measurements of the surface coating layer [15]. The specimens with the highest surface roughness measured by a surface roughness tester type (TR210) were IN 738 LC (10 Al+90 Al_2O_3) and IN 738 LC (40 Al+60 Al_2O_3), respectively, while AFM (Atomic Force Microscopy, Park, NX10, Korea) readings show that IN 738 LC (10 Al+90 Al_2O_3) has the highest surface roughness.

Table 3

Coating Surface Roughness

Coated Sample	Roughness (μm)	Average roughness by AFM(nm)
IN 738 LC (10 Al+90 Al_2O_3)	6.367	28.2
IN 738 LC (40 Al+60 Al_2O_3)	5.752	15.5

IN 738 LC (40 Al+60 Al_2O_3) sample had lower surface roughness as measured by a surface roughness tester. Fig. 2 shows the atomic force microscope analysis results.

Slurry coating process has been used to reduce oxidation occurred in turbine blade and includes coating materials and coating process. After finishing of grinding, cleaning, polishing, then, the powders (Al+Al_2O_3) were wetly mixed in two different proportions, (10 Al+90 Al_2O_3) and (40 Al+60 Al_2O_3) by using planetary automatic balls mill equipped with five steel balls differ in diameter to mix and refine metal powder for 3 hours.

Table 1

Chemical Analysis of the Used IN 738 LC

Element	Titanium (Ti)	Chromium (Cr)	Iron	Cobalt (Co)	Niobium (Nb)	Molybdenum (Mo)	Tantalum (Ta)	Tungsten (W)	Nickel (Ni)	LEC
Wt. %	3.2	6.1	0.09	7.3	0.5	1.4	1.8	2.8	Base	3.1

Wt.: Weight Percentage

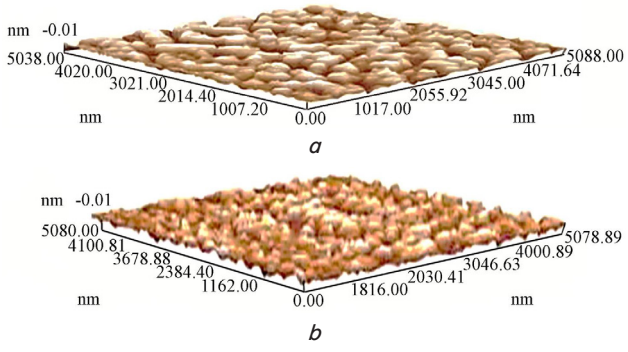

Fig. 2. Atomic force microscope analysis: *a* – IN 738 LC (10 Al+90 Al_2O_3); *b* – IN 738 LC (40 Al+60 Al_2O_3)

Ethanol was used as a mixing medium of wet mixing. then the binder was prepared and two types of binder were used after conducting the contact angle test was concluded that PVA is better than PEG (India). The 5 ml of PVA with an initial concentration of PVA<4.0 M and a limited final pH value of ≈8.0 is added to the powder mixed with the magnetic stirrer device , then the sample is immersed in the mixture and then the sample is dried. After the completion of coating process all the specimens are put in vacuum furnace (Electrical Tube Furnace Type MTI-(GSL1600X)) at 35 °C and 1000 °C for an hour once and for two hours again.

5. Result of study the thermally coated by Al_2O_3 using slurry coating

5. 1. The Oxidation of coating layer at isothermal oxidation

In order to study the oxidation resistance of Inconel 738 LC with and without coating, cyclic oxidation at high temperature was carried out. The tests were carried for 1000 °C at 55 oxidation at high temperature 1000 °C was carried out at 55 hours in argon atmosphere, every 5 hours after the oxidation for the tested specimens are weighted, where the test are in air atmosphere. Specimens with and without coating were accurately weighed. The oxidation resistance of the specimens was tested by heating them in a furnace at test temperatures and weighing them every 5 hours. And weighting them and recorded the amount of the change in weight as result of oxidation.

The uncoated IN 738 LC alloy and alloy with coverings is shown in Fig. 3 in the kinetics of oxidation. The maximum oxidation rate at 1100 °C was the uncoated alloy. The weight gain in both coatings in IN 738 LC (10 Al+90 Al_2O_3) and in IN 738 LC (40 Al+60 Al_2O_3) is not significantly different at 1100 °C. At 1000 °C, however, the oxidation percentages of the alloy IN 738 LC were higher than that for IN 738 LC (40 Al+60 Al_2O_3). A substantial mass loss at 1000 °C affected the uncoated alloy.

For kinetical identification in dry air in the temperature range of 1100 °C for 55 hours in the 5-hour cycle specified weight variations of the uncoated IN 738 LC alloy have been recorded as a function of time, according to Fig. 3, in dry air. The initial kinetic is quick, but with time the rate of weight change is gradual. The kinetics may be explained by considering the constant time or growth rate (n). Growth rate (n) can be determined using the equation below [17, 19]:

$$W/A=kt^n, \quad (1)$$

where $\Delta W/A$ is the specific change in weight, k is the rate constant, t is the oxidation time, and n is the growth-rate time constant.

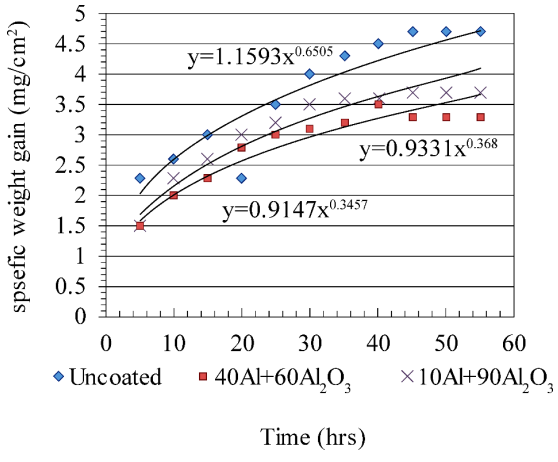

Fig. 3. Parabolic fitted results of specific weight change vs. time plotted for uncoated and coated IN 738 superalloy with Al+Al_2O_3 diffusion coating after cyclic oxidation in air at temperatures between 1100 °C for 55 hrs at 5hrs

The k_P value is then squared to give k_P in units of $(mg^2 \cdot cm^{-4})$/hr, as displayed in the expression below:

$$(\Delta W/A)^2=k_P t. \quad (2)$$

It should be noted that the other values of n and k_P in this research are determined by employing the same procedure as mentioned above. Data from the experiments revealed that a parabolic oxidation rate (k_P) obeys an Arrhenius equation of the form:

$$k_P=k_o \exp(-Q/RT), \quad (3)$$

where k_P denotes the parabolic oxidation rate, k_o denotes the pre-exponential factor, Q denotes the activation energy, T denotes the temperature, and R denotes the universal gas constant (8.33 J/K·mol).

If n is greater or less than 0.5, the kinetic oxidation doesn't follow the simple parabolic model, meaning that oxidation rates are faster. The parabolic rate is exceeding n>0.5, for example, while n is greater than 0.5, the parabolic rate is less than parabolic (sub-parabolic). Table 4 shows n values and parabolic oxidation rate constants k_P for cyclic oxidation.

Table 4

n values and parabolic oxidation rate constants k_P for cyclic oxidation

Alloy	n values	k_P $(mg^2 \cdot cm^{-4})$/sec.
Uncoated	0.6505	$6.94 \cdot 10^{-11}$
IN 738 LC (10 Al+90 Al_2O_3)	0.368	$1.00 \cdot 10^{-10}$
IN 738 LC (40 Al+60 Al_2O_3)	0.3457	$0.7 \cdot 10^{-10}$

5. 2. Effect of Al_2O_3 and Al additions on oxidation resistance

The results show that sub-parabolize mechanisms (short circuits) can be found. An oxide layers cracking, which sud-

denly increases the surface area in contact with oxygen and speeds up the oxidation kinetic, may explain the difference between the theoretical value n=0.5 as indicated in a previous study [20, 21].

Following oxidation, Fig. 4 demonstrates the uncoated alloy's cross-sectional morphology. Due to its low Al content, the uncoated alloy does not compose a protective Al_2O_3 scale. The surface at 1000 to 1100 °C was instead mixed with NiO and Cr_2O_3, and Al only forms inner oxide during the oxidation process.

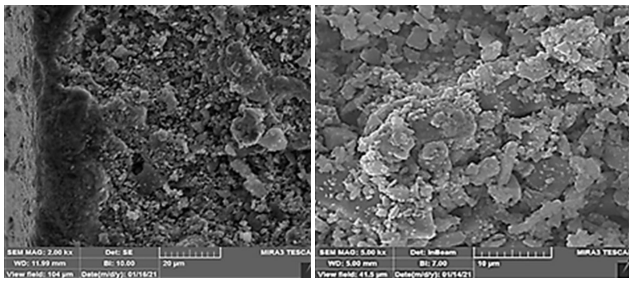

a *b*

Fig. 4. Scanning Electron Microscope micrographs of the coated specimens with (10 Al+90 Al_2O_3) Diffusion Coating after Oxidation: *a* — 20 μm in magnification; *b* — 10 μm in magnification

EDX analysis results of the coated specimens with (10 Al+90 Al_2O_3) propagation coating after the cyclic oxidation are depicted in Fig. 5.SEM micrographs of the coated specimens with (40 Al+60 Al_2O_3) propagation coating after the cyclic oxidation are demonstrated in Fig. 5.

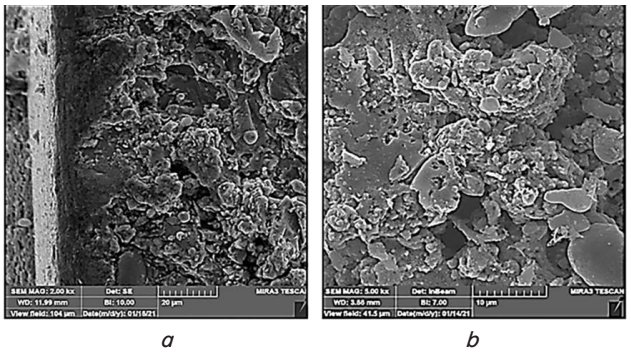

a *b*

Fig. 5. Scanning Electron Microscope micrographs of the coated specimens with (40 Al+60 Al_2O_3) Diffusion Coating after the Cyclic Oxidation: *a* — 20 μm magnification; *b* — 10 μm magnification

5. 3. Two ratio of aluminized coating for oxidation resistance

Fig. 6 depicts the EDX analysis results of the coated samples with (40 Al+60 Al_2O_3) propagation coating after cyclic oxidation. Fig. 7 SEM micrographs of the uncoated specimens after the Cyclic Oxidation, while Fig. 8 displays the EDX analysis results of the uncoated specimens after the cyclic oxidation.

XRD results of specimens that are exposed to oxidation at 1100 °C for a period of 50 hrs can be found in Fig. 9–11. The oxides constituted on the alloy's uncoated surface are pores that are badly connected to them Fig. 9. The surface at 1000 to 1100 °C was instead mixed with NiO and Cr_2O_3, and Al only forms inner oxide during the oxidation process.

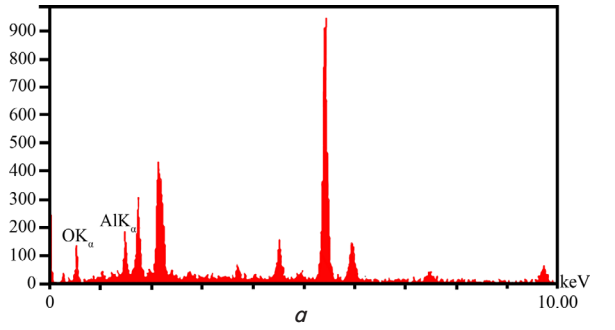

a

Elt	Line	Int	Error	K	Kr	W%	A%	ZAF	Formula	Ox%	Pk/Bg
O	Ka	158.9	3.7629	0.3584	0.1926	50.36	63.12	0.3824		0.00	66.62
Al	Ka	267.7	28.6453	0.6416	0.3448	49.64	36.88	0.6946		0.00	15.98
				1.0000	0.5374	100.00	100.00			0.00	

b

Fig. 6. Electron dispersion analysis results: *a* — coated specimens with (40 Al+60 Al_2O_3) diffusion coating after the cyclic oxidation; *b* — amounts of the calculated elements

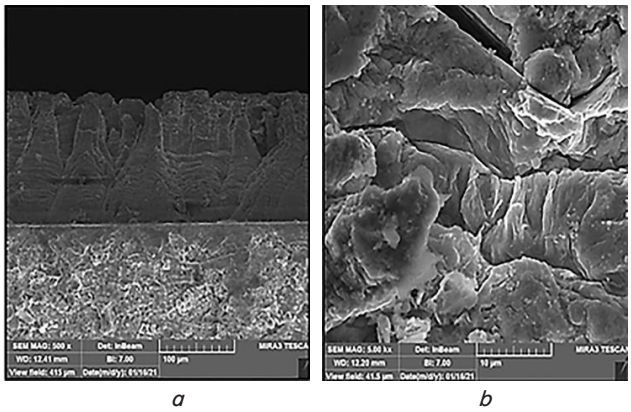

a *b*

Fig. 7. Scanning Electron micrographs of the Uncoated specimens after the Cyclic Oxidation: *a* — 100 μm magnification; *b* — 10 μm magnification

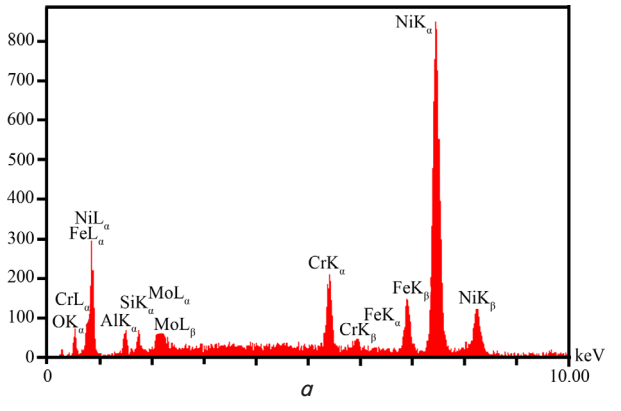

a

Elt	Line	Int	Error	K	Kr	W%	A%	ZAF	Formula	Ox%	Pk/Bg
O	Ka	73.0	6.0890	0.0191	0.0169	4.44	13.47	0.3799		0.00	24.98
Al	Ka	84.1	3.1950	0.0234	0.0206	5.99	10.77	0.3447		0.00	7.49
Si	Ka	43.5	3.1950	0.0123	0.0108	2.38	4.11	0.4559		0.00	3.95
Cr	Ka	347.9	3.5421	0.1200	0.1059	10.25	9.56	1.0337		0.00	7.51
Fe	La	36.6	6.0890	0.0097	0.0085	1.27	1.10	0.6753		0.00	9.33
Ni	Ka	2050.1	3.5421	0.7790	0.6877	70.79	58.52	0.9714		0.00	31.41
Mo	La	125.2	3.1950	0.0365	0.0322	4.88	2.47	0.6603		0.00	4.38
				1.0000	0.8828	100.00	100.00			0.00	

b

Fig. 8. Electron Dispersion Analysis Results of the Uncoated samples after the Cyclic Oxidation (*a*); Amounts of the calculated elements (*b*)

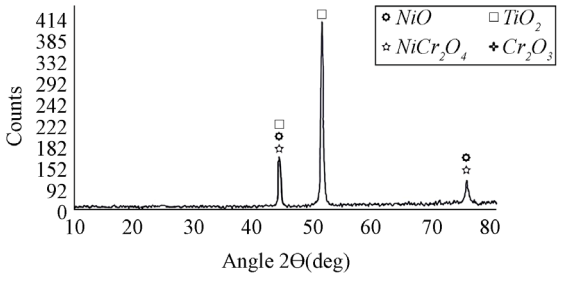

Fig. 9. X-ray Diffraction Analysis Results of the Uncoated Specimens after the Cyclic Oxidation

The link between the layer and the substratum is strong for coated samples and the thickness of all aluminum coatings is consistent. The coatings do not include cracks or voids, Fig. 10, 11.

The Al concentration declines gradually from the cover surfaces to the substrate, but drops sharply at the coat interface. The composition of the cover is therefore a counter spread process for the propagates of alloy components from the internal to the external layer, as Al stays on the surface and propagates into the substrate, as involved in the Massalski analysis [29]. Additionally, slurry aluminide coatings containing 1 wt. % in Si are very resistant to high temperature oxidation under both isothermal and cyclic conditions.

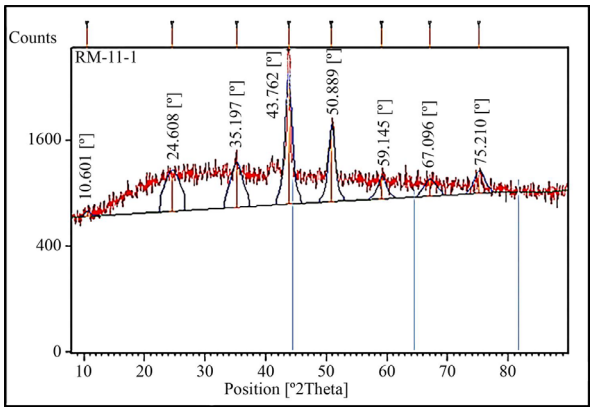

a

Structure Plot | Fourier Map | Distances and Angles

Pattern List | Scan List | Peak List | Anchor Scan Data | Object Inspector | Quantification | Refinement Control

No.	Pos. [°2Th.]	d-spacin...	Rel. In...	FWHM [°...	Matched by	Area [cts*°2...	Backgr.[cts]	Height [cts]
1	10.6009	8.34544	2.77	0.9840		49.49	656.00	50.98
2	24.6084	3.61769	23.27	3.1488		1331.12	709.00	428.55
3	35.1971	2.54985	26.09	2.3616		1119.33	749.74	480.48
4	43.7617	2.06864	100.00	1.1808		2145.54	782.00	1841.98
5	50.8895	1.79438	51.33	1.1808		1101.37	809.00	945.55
6	59.1446	1.56212	12.99	1.5744		371.53	840.69	239.22
7	67.0959	1.39502	9.67	2.3616		415.13	870.72	178.20
8	75.2100	1.26234	10.15	1.9200		478.73	901.00	187.00

b

Fig. 10. X-ray Diffraction Analysis Results:
a – Coated Specimens with (10 Al+90 Al_2O_3) Diffusion Coating after the Cyclic Oxidation; *b* – peak list

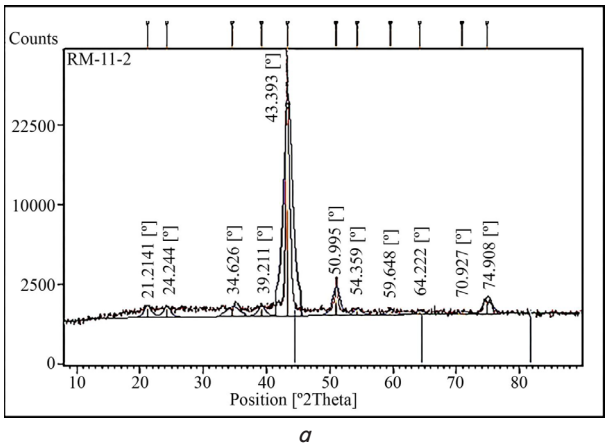

a

Structure Plot | Fourier Map | Distances and Angles

Pattern List | Scan List | Peak List | Anchor Scan Data | Object Inspector | Quantification | Refinement Control

No.	Pos. [°2Th.]	d-spacin...	Rel. In...	FWHM [°...	Matched by	Area [cts*°2...	Backgr.[cts]	Height [cts]
1	21.2137	4.18831	1.90	1.1808		550.92	845.00	472.97
2	24.2444	3.67117	1.69	1.1808		490.40	852.69	421.01
3	34.6257	2.59061	1.52	2.3616		880.75	879.00	378.07
4	39.2106	2.29761	1.73	1.1808		499.84	891.00	429.12
5	43.3934	2.08534	100.00	1.1808		28944.61	901.00	24849.43
6	50.9950	1.79091	5.28	1.1808		1529.04	921.00	1312.70
7	54.3594	1.68775	1.01	1.1808		291.43	929.00	250.20
8	59.6477	1.55014	0.80	1.1808		231.14	942.75	198.44
9	64.2216	1.45033	0.65	1.1808		188.93	954.00	162.20
10	70.9271	1.32878	0.42	1.5744		163.04	971.00	104.98
11	74.9083	1.26568	2.17	1.4400		1035.10	981.00	539.11

b

Fig. 11. X-Ray Diffraction Analysis Results:
a – Coated Specimens with (40 Al+ 60 Al_2O_3) Diffusion Coating after the Cyclic Oxidation; *b* – peak list

6. Discussion of study results of oxidation

Nickel-based superalloys have found extensive applications in gas turbine industries due to their excellent thermo-mechanical properties. The corrosion of turbine blades induced by high temperatures is an extreme danger to the performance of electrical gas power plants, resulting in massive economic losses. Slurry coating process has been used to reduce oxidation occurred in turbine blade and includes coating materials and coating process

During isothermal cyclic oxidation, the aluminized coatings create a highly thick and continuous Al_2O_3 scale on top of the coats.

Their effective temperature anti-oxidation is raised to 1100 °C and they have outstanding high temperature oxidation resistance (Fig. 7, *b*, 8, *b*).

Therefore aluminized coatings for turbine blades produce high resistance against oxidation at overheated condition.

The thermal coating has a good resistance to oxidation because of exclusive α-Al_2O_3 production at 1100 °C, due mostly to the presence of large amounts of aluminum (Fig. 9, *b*, 10, *b*).

However testing of coated turbine blades for other application required a temperature more than 1100 °C. Additionally, for future work, testing coating resistance for other applications with other coating materials at overheated temperature conditions for improving such alloys against oxidation.

7. Conclusions

1. Oxidation rates of Inconel 738LC specimens increase with time and temperature as the oxide layer scales, becoming porous and weakly adhering to the substrate's surface. During isothermal cyclic oxidation, the aluminized coatings create a highly thick and continuous Al_2O_3 scale on top of the coats. Their effective temperature anti-oxidation is raised to 1100 °C and they have outstanding high temperature oxidation resistance.

2. Alloys with both Al_2O_3 and Al additions have reported positive synergistic effect of the Al_2O_3 and Al additions on oxidation resistance. Slurry aluminide coatings containing 1 wt. % in Si are very resistant to high temperature oxidation under both isothermal and cyclic conditions.

3. The oxidation resistance of the aluminized coating (10 Al+90 Al_2O_3) was comparable to that of the (40 Al+ +60 Al_2O_3) coating. Furthermore, it still retained high oxidation resistance at 1100 °C due to the makeup of Al_2O_3 scale and the coating contains a high percentage of Al. The $NiCrAl_2O_3$ thermal coating has a good resistance to oxidation because of exclusive α-Al_2O_3 production at 1100 °C, due mostly to the presence of large amounts of aluminum.

Acknowledgement

The authors would like to express their gratitude for the support provided by the University of Baghdad, Iraq.

References

1. Basuki, E. A., Prajitno, D. H., Muhammad, F. (2017). Alloys developed for high temperature applications. AIP Conference Proceedings. doi: https://doi.org/10.1063/1.4974409
2. Long, H., Mao, S., Liu, Y., Zhang, Z., Han, X. (2018). Microstructural and compositional design of Ni-based single crystalline superalloys – A review. Journal of Alloys and Compounds, 743, 203–220. doi: https://doi.org/10.1016/j.jallcom.2018.01.224
3. Goodfellow, A. J. (2018). Strengthening mechanisms in polycrystalline nickel-based superalloys. Materials Science and Technology, 34 (15), 1793–1808. doi: https://doi.org/10.1080/02670836.2018.1461594
4. Donachie, M. J., Donachie, S. J. (2002). Superalloys.ASM International.doi: https://doi.org/10.31399/asm.tb.stg2.9781627082679
5. Birks, N., Meier, G. H., Pettit, F. S. (2006). Introduction to the High Temperature Oxidation of Metals. Cambridge University Press. doi: https://doi.org/10.1017/cbo9781139163903
6. Jokar, A., Ghadami, F., Azimzadeh, N., Doolabi, D. S. (2021). Slurry Aluminizing Process of the Internal Passageways of Gas Turbine Blades: Investigation of High-Temperature Oxidation Behavior at 1000 °C. SSRN Electronic Journal.doi: https://doi.org/10.2139/ssrn.3967530
7. Shao, Y., Xu, J., Wang, H., Zhang, Y., Jia, J., Liu, J. et. al. (2019).Effect of Ti and Al on microstructure and partitioning behavior of alloying elements in Ni-based powder metallurgy superalloys. International Journal of Minerals, Metallurgy, and Materials, 26 (4), 500–506. doi: https://doi.org/10.1007/s12613-019-1757-1
8. Zakeri, A., Masoumi Balashadehi, M. R., Sabour Rouh Aghdam, A. (2021). Development of hybrid electrodeposition/slurry diffusion aluminide coatings on Ni-based superalloy with enhanced hot corrosion resistance. Journal of Composites and Compounds, 2 (5), 1–8. doi: https://doi.org/10.52547/jcc.3.1.1
9. Maniam, K. K., Paul, S. (2021). Progress in Novel Electrodeposited Bond Coats for Thermal Barrier Coating Systems. Materials, 14 (15), 4214.doi: https://doi.org/10.3390/ma14154214
10. Sims, C. T., Stoloff, N. S., Hagel, W. C. (Eds.) (1987). Superalloys II. Wiley.
11. Goebel, J. A., Pettit, F. S., Goward, G. W. (1973). Mechanisms for the hot corrosion of nickel-base alloys. Metallurgical Transactions, 4 (1), 261–278. doi: https://doi.org/10.1007/bf02649626
12. Gupta, A. K., Immarigeon, J. P., Patnaik, P. C. (1989). A review of factors controlling the gas turbine hot section environment and their influence on hot salt corrosion test methods. High Temperature Technology, 7 (4), 173–186. doi: https://doi.org/10.1080/02619180.1989.11753435
13. Fuhui, W., Hanyi, L., Linxiang, B., Weitao, W. (1989). Hot corrosion of yttrium-modified aluminide coatings. Materials Science and Engineering: A, 120-121, 387–389. doi: https://doi.org/10.1016/0921-5093(89)90792-2

14. Gleeson, B., Cheung, W. H., Costa, W. D., Young, D. J. (1992). The hot-corrosion behavior of novel CO-deposited chromium-modified aluminide coatings. Oxidation of Metals, 38 (5-6), 407–424. doi: https://doi.org/10.1007/bf00665662
15. He, Y.-R., Rapp, R. A., Tortorelli, P. P. (1997). Oxidation-resistant Ge-doped silicide coating on Cr-Cr2Nb alloys by pack cementation. Materials Science and Engineering: A, 222 (2), 109–117. doi: https://doi.org/10.1016/s0921-5093(96)10516-5
16. Hsu, H.-W., Tsai, W.-T. (2000). High temperature corrosion behavior of siliconized 310 stainless steel. Materials Chemistry and Physics, 64 (2), 147–155. doi: https://doi.org/10.1016/s0254-0584(99)00264-3
17. Zhou, C., Xu, H., Gong, S., Yang, Y., Young Kim, K. (2000). A study on aluminide and Cr-modified aluminide coatings on TiAl alloys by pack cementation method. Surface and Coatings Technology, 132 (2-3), 117–123. doi: https://doi.org/10.1016/s0257-8972(00)00911-7
18. Koo, C. H., Yu, T. H. (2000). Pack cementation coatings on Ti3Al–Nb alloys to modify the high-temperature oxidation properties. Surface and Coatings Technology, 126 (2-3), 171–180. doi: https://doi.org/10.1016/s0257-8972(00)00546-6
19. Kassim, S. A., Shukri, N. M. M., Zubir, S. A., Seman, A. A., Abdullah, T. K. (2021). Si-Mo-Modified Aluminide Slurry Coating For High Temperature Protection Of Austenitic Stainless Steel. Malaysian Journal of Microscopy, 17 (2).Available at: https://malaysianjournalofmicroscopy.org/ojs/index.php/mjm/article/view/547
20. Eliaz, N., Shemesh, G., Latanision, R. M. (2002). Hot corrosion in gas turbine components. Engineering Failure Analysis, 9 (1), 31–43. doi: https://doi.org/10.1016/s1350-6307(00)00035-2
21. Visuttipitukul, P., Limvanutpong, N., Wangyao, P. (2010). Aluminizing of Nickel-Based Superalloys Grade IN 738 by Powder Liquid Coating. MATERIALS TRANSACTIONS, 51 (5), 982–987. doi: https://doi.org/10.2320/matertrans.m2009382
22. Shmorgun, V. G., Bogdanov, A. I., Kulevich, V. P., Iskhakova, L. D., Taube, A. O. (2021). Microstructure and phase composition of diffusion coating formed in NiCr alloys by hot-dip aluminizing. Surfaces and Interfaces, 23, 100988.doi: https://doi.org/10.1016/j.surfin.2021.100988
23. Keyvani, A. (2015). Microstructural stability oxidation and hot corrosion resistance of nanostructured Al2O3 /YSZ composite compared to conventional YSZ TBC coatings. Journal of Alloys and Compounds, 623, 229–237. doi: https://doi.org/10.1016/j.jallcom.2014.10.088
24. Lorenzo-Bañuelos, M., Díaz, A., Rodríguez, D., Cuesta, I. I., Fernández, A., Alegre, J. M. (2021). Influence of Atmospheric Plasma Spray Parameters (APS) on the Mechanical Properties of Ni-Al Coatings on Aluminum Alloy Substrate. Metals, 11 (4), 612. doi: https://doi.org/10.3390/met11040612
25. Keyvani, A., Saremi, M., Sohi, M. H. (2011). An investigation on oxidation, hot corrosion and mechanical properties of plasma-sprayed conventional and nanostructured YSZ coatings. Surface and Coatings Technology, 206 (2-3), 208–216. doi: https://doi.org/10.1016/j.surfcoat.2011.06.036
26. Vadayar, K. S., Rani, S. D. (2013). Hot corrosion behaviour of nickel based superalloys. International Journal of Applied Research in Mechanical Engineering, 2 (4), 223–227. doi: https://doi.org/10.47893/ijarme.2013.1090
27. Pakseresht, A. H., Javadi, A. H., Bahrami, M., Khodabakhshi, F., Simchi, A. (2016). Spark plasma sintering of a multilayer thermal barrier coating on Inconel 738 superalloy: Microstructural development and hot corrosion behavior. Ceramics International, 42 (2), 2770–2779. doi: https://doi.org/10.1016/j.ceramint.2015.11.008
28. Massalski, T. B. (1988). Binary alloy phase diagrams. ASM Handbook, 114–125.